9C.4   **Asymmetric Structures in a Sheared TC and their Effect on the Energy Content of the Eyewall**

Klaus P. Dolling and Gary M. Barnes

University of Hawaii

1. Introduction

The cause of intensity change of tropical cyclones (TCs) continues to be a major challenge for the meteorological community (Marks et al. 1998, AMS statement on Hurricane Research and Forecasting 2006, National Science Board Report 2006, Holland and Lukas 2006). Intensity change may be defined as a deepening or filling of central sea-level pressure or an increase or decrease of the maximum sustained winds in the eyewall. In 2001 the National Oceanic and Atmospheric Administration and the National Aeronautical and Space Administration marshaled their resources to collect a more complete dataset that may be utilized to address the evolutionary aspects of a TC.

———————————————————————

Corresponding author: K. P. Dolling
Department of Meteorology, University of Hawaii
2525 Correa Road, Honolulu, Hawaii 96822
dolling@hawaii.edu

The unprecedented sampling of TC Humberto during the Convection and Moisture Experiment (CAMEX-4) provides an opportunity to examine the details of changes in intensity as Tropical Storm Humberto intensifies to a category 2 hurricane and then weakens to a category 1. Rarely do we get a view of storm evolution over 3 successive days with multiple aircraft, the deployment of over 200 Global Positioning System dropwindsondes (GPS sondes), and airborne expendable bathythermographs (AXBTs).

Frank (1977) successfully identified the synoptic-scale features of a mature typhoon by compositing the observations from hundreds of TCs. Instead of gathering many storms of different intensity and spatial scale, in this study we examine the evolution of an individual storm as it progresses through the early stages of development. Using methods similar to those of Frank

(1977), we composite GPS sondes jettisoned over 3 to 4 hours for each day.

The observations of Hurricane Humberto provide an opportunity to investigate the structure of a storm that forms, intensifies, and weakens at higher latitudes. During the peak intensity and the period of filling on the 23rd (Fig. 1), Humberto is in a high shear environment, traveling over large sea surface temperature (SST) gradients.

Equivalent potential temperature (θ_e) is related to the total energy content of an air parcel. It is useful in that it is a conserved variable in the absence of energy gains from the sea surface and energy losses from radiation which are generally small over the typical composite time. Equivalent potential temperature has been correlated with intensity through both empirical and theoretical arguments (Malkus and Riehl 1960, Emanuel 1986).

Mapping the location of the radius of maximum wind (RMW) in concert with detailed maps of θ_e in the boundary layer help to clarify exactly where large gradients of θ_e exist. Past research indicates that fluxes of sensible and latent heat from the ocean surface increase greatly near the eyewall in response to higher wind speeds (Riehl and Malkus 1961, Hawkins and Rubsam 1968, Wroe and Barnes 2003). The Humberto data will help identify if θ_e increases occur at further distances from the eye and if this air is advected into eyewall or if the increases occur near and under the eyewall.

At 09/22/01 0600 UTC Humberto was a 1010 hPa tropical depression. Its central pressure would continue to decline at a steady rate until late on the 23rd when the aircraft left the storm on the second day of sampling. Late on the 23rd as the storm traveled north northeast at 5-6 m s^{-1}, the northern half of the TC circulation (including the eye-eyewall) was traveling over a large gradient in SSTs with cold temperatures to the north (Fig. 2). The main questions we will examine are: (a) why does Humberto continue to intensify when the northern half of circulation is over cold SSTs? (b) In a sheared asymmetric TC, is there an inflow channel that is supplying the eyewall with its high energy content? (c) How well does an energy budget using data from GPS sondes compare with the bulk aerodynamic equations?

2. Data and Methodology

The two WP-3Ds sampled the inner core out to about two degrees latitude from the storm center making three passes each through the circulation center. The DC-8 flew a similar pattern to the WP-3D's except with a slightly wider sampling area. The ER-2 sampled the storm out to about four degrees from the circulation center. All the aircraft jettisoned GPS sondes from different altitudes, sampling the entire troposphere with the highest resolution in the lower 2 km. Both WP-3Ds also deployed airborne expendable bathythermographs (AXBT's) allowing for a detailed map of the SSTs. GPS sondes have a 2 Hz sampling rate and a vertical resolution of ~7 m in the lower troposphere. Typical errors for pressure, temperature, and relative humidity are 1.0 hPa, 0.2 °C, and <5%, respectively (Hock and Franklin 1999).

On the 23rd 100 GPS sondes were jettisoned. Figure 3 shows the locations of the sondes relative to the TC center. The horizontal resolution on the 23rd was about 20 km near the eyewall with a lower resolution farther outward from the circulation center.

3. Preliminary Results

On the 23rd, the vertical shear of the horizontal wind (VWS) was 11 m s^{-1} at 45° and the eyewall (Fig. 4) has convection downshear and left of the shear vector similar to past studies (Eastin et al. 2005, Black et al. 2002). The 250 m radial winds and streamlines (Fig. 5) have a marked asymmetry with strong inflow and confluence to the north and east of the circulation center and outflow with diffluence to the south and west of the circulation center. To the north of the circulation center are bands of convection (Fig. 6) and a rainband is present in the radar imagery (not shown) trailing off to the southeast of the circulation center. A storm-scale view of the θ_e at 50 m (Fig 7.) displays strong asymmetries. High θ_e of 354 K is ingested into the rainband to the southeast associated with confluence in the streamlines. To the north of the circulation center where convective bands occur θ_e drops to 340-347 K. The low θ_e encircles more then half of the storms' circulation.

A close up view of the eyewall at 200 m displays an inflow trajectory (Fig. 8), for the boundary layer, starting at sounding 1 where θ_e is at a minimum to sounding 5 as θ_e increased from 345 K to

351 K before entering the eyewall. Warmer θ_e to the northwest of the RMW is cooled as a convective downdraft from the eyewall spills into the boundary layer. Humberto is intensifying in a dry environment based on the environmental relative humidity from the statistical hurricane intensity prediction scheme (SHIPS, DeMaria and Kaplan 1999). The 700-300 hPa level has a relative humidity of 45% for the three days of sampling. The entrainment of dry air causes cool downdrafts which must be overcome so that θ_e can recover before moving up the eyewall column.

An energy budget is calculated from sounding 1 to sounding 5 to compare the energy gain from the bulk aerodynamic equations using the transfer coefficients from Fairall et al. (2003) with the energy gain observed from the GPS dropsondes in our composite fields. The equation for the energy budget is:

$$V\frac{\partial \bar{\theta}_e}{\partial \eta} + w\frac{\partial \bar{\theta}_e}{\partial z} = -\frac{\partial (\overline{w'\theta_e'})}{\partial z}$$

where V = horizontal velocity along the inflow trajectory, η = the distance along the trajectory, w = vertical velocity, and z = height. The first term on the lhs of the equation is the product of the velocity along the inflow trajectory and the gradient of θ_e estimated along the trajectory. The second term on the lhs of the equation is the product of the vertical velocity and the vertical gradient of θ_e. If convergence is present along the inflow trajectory, it can compress and raise the height of the mixed inflow layer. This is not an increase in the energy content of the inflow but instead a redistribution of the energy. The first term on the rhs of the equation corresponds to the subgrid-scale fluxes at the air-sea interface and the transfer of energy through the top of the layer of air being examined. The full equation may be found in Wroe and Barnes (2003). Terms that have been scaled out include: the storage term as Humbertos central pressure changes by only a few hPa throughout the 3-4 hours of sampling, radiative divergence which is minimal for the composite time, and dissipative heating, most of which has been observed to be absorbed into the oceanic mixed layer (Zhang 2010).

Observations of the 10 m total wind speed, temperature, specific humidity, and SSTs are used to calculate the fluxes from the sea surface. From

sounding 1 to 2 the wind speeds average 36 m s^{-1}, the temperature difference is approximately 3 K and the specific humidity difference is just under 5 g kg^{-1}. There is a slight amount of convergence but sounding 1 is fairly well mixed so it does not affect the total energy content (Fig. 9a). The total energy needed from sounding 1 to 2 is 833 W m^{-2}, while estimates from the bulk aerodynamic equations are 797 W m^{-2} resulting in a 4.5% error. From sounding 2 to 3 the average wind speed is 25 m s^{-1}, the temperature difference is just under 3 K, and the specific humidity difference is about 6 g kg^{-1}. The total energy needed from the Humberto composite with convergence in the layer (Fig. 9b) is 559 W m^{-2} and from the bulk aerodynamic equations is 626 W m^{-2}, resulting in an 11% error. For sounding 3 to 4, the total wind speed is 25 m s^{-1}, temperature difference is 3 K, and the specific humidity difference is 5.4 K g kg^{-1}. There is net divergence along this trajectory (Fig. 9c) resulting in 621 W m^{-2} from the Humberto composite and 570 W m^{-2} from the bulk aerodynamic equations. This constitutes a 9% error. For the last leg of the trajectory (sounding 4-5), the average

total wind speed is 33 m s^{-1}, the temperature difference is 2.8 K and the specific humidity difference is about 5 g kg^{-1}. The energy needed for the Humberto composite with net divergence in the layer (Fig. 9d) is 933 W m^{-2} and from the bulk aerodynamic equations is 711 W m^{-2}. This results in a 28% error.

The inflow column from the Humberto composite from sounding 1 to 5 receives an average of 715 W m^{-2}. Estimates from the bulk aerodynamic equations are 676 W m^{-2}. The total error is 6% and well within the 20% uncertainty of the transfer coefficients at these higher wind speeds.

4. Conclusions

As Humberto moves to the north-northeast it continues to intensify even though cold SSTs are under the northern half of the circulation. Emanuel (1986) and Malkus and Riehl (1960) have shown the θ_e of the eyewall column is correlated with intensity. The analysis of Humberto reveals that the high θ_e entering the eyewall is a result of an asymmetric wind field and an inflow trajectory that moves over warmer SSTs south of the circulation center.

Following this inflow trajectory the energy of the column recovers from the low θ_e in a convective downdraft from the eyewall. An energy budget for the inflow shows near balance within 6%. The inflow trajectory investigated has a long residence time in high winds with no convective downdrafts allowing it to pick up the necessary energy to feed the eyewall and is partially the cause for the continued intensification until the end of sampling late on the 23rd. Humberto begins to weaken as the inflow trajectory investigated travels over cooler SSTs a few hours later.

4. References

American Meteorological Society Statement on Hurricane Research and Forecasting, 2000: *Bull. Amer. Meteor. Soc.*, **81**, 1341- 1346.

Black, M. L., J. F. Gamache, F. D. Marks Jr., C. E. Samsury, and H. E. Willoughby, 2002: Eastern Pacific Hurricanes Jimena of 1991 and Olivia of 1994: The effect of vertical wind shear on structure and intensity. *Mon. Wea. Rev.*, **130**, 2291-2312.

DeMaria,M., M. and J. Kaplan, 1994: A statistical hurricane intensity prediction scheme (SHIPS) for the Atlantic Basin. *Wea. Forecasting*, **9**, 209-220.

Eastin, D. E., W. M. Gray, and P. G. Black, 2005: Buoyancy of convective vertical motions in the inner core of intense hurricanes. Part II: Case studies. *Mon. Wea. Rev.*, **133**, 209-227.

Emanuel, K. A., 1986: An air-sea interaction theory for tropical cyclones. Part I: Steady-state maintenance. *J. Atmos. Sci.*, **43**, 585-604.

Fairall, C. W., E. F. Bradley, J. E. Hare, A. A . Grachev, and J. B. Edson, 2003: Bulk parameterization of air-sea fluxes: Updates and verification for the COARE algorithm. *J. Climate.*, **16**, 571-591.

Frank, W. M., 1977: The structure and energetics of the tropical cyclone. I. Storm structure. *Mon. Wea. Rev.*, **105**, 1136-1150.

Hawkins, H. F., and D. T. Rubsam, 1968: Hurricane Hilda, 1964, II. Structure and budgets of the hurricane on October 1, 1964. *Mon. Wea. Rev..*, **96**, 617-636.

Hock, T. F., and J. L. Franklin, 1999: The NCAR GPS dropwindsonde. *Bull. Amer. Meteor. Soc.*, **80**, 407-420.

Holland, G. J., and R. Lukas, 2006: Program for improvements to hurricane intensity forecasts and impacts projections (HiFi). Report available from authors via web.

Marks, F.D.Jr., L. K. Shay, and PDT-5, 1998: Landfalling tropical cyclones: Forecast problems and associated research opportunities. *Bull. Amer. Meteor. Soc.*, **79**, 305-323.

Malkus, J. S., and H. Riehl, 1960: On the dynamics and energy transformation in steady-state hurricanes. *Tellus*, **12**, 1-20.

National Advisory Board, 2007: Hurricane Warning: The critical need for a national hurricane research initiative. [available from NSF.]

Wroe, R. and G. M. Barnes, 2003: Inflow layer energetics of Hurricane Bonnie (1998) near landfall. *Mon. Wea. Rev.*, **131**, 1600-1612.

Zhang, J. A., 2010: Estimation of dissipative heating using lowlevel in situ aircraft observations in the hurricane boundary layer. J. Atmos. Sci., 67, 1853–1862.
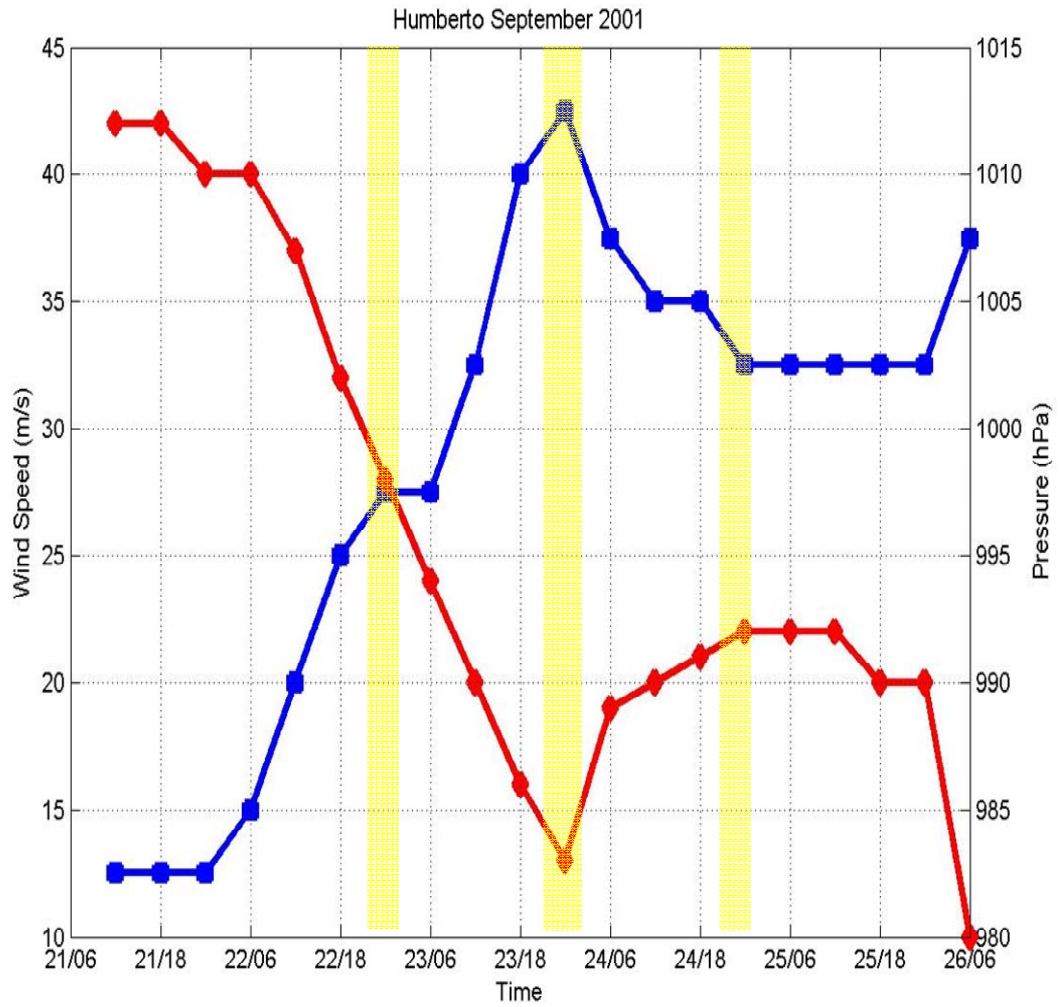
Fig. 1"Best Track" 1-minute sustained 10 m wind speed and surface pressure data for Humberto. Red line marks the pressure line with red diamonds showing the time of each observation. Blue line marks the 10 m wind speed with blue squares marking the time of each observation. Light yellow rectangles show times of observation for each of the three days.

Sea Surface Temperature
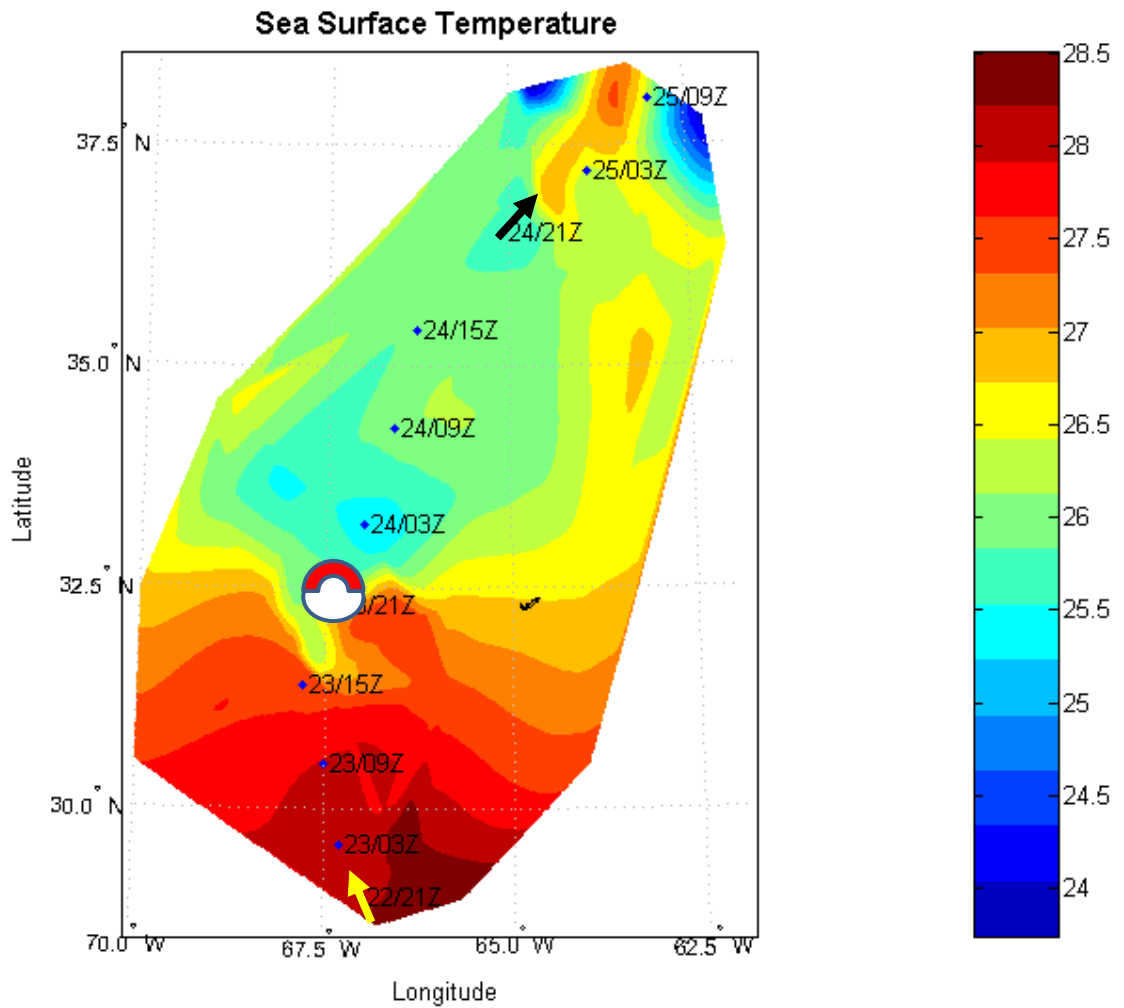
Fig. 2 Map of sea surface temperatures (°**C**) from the AXBT's. AXBT's were deployed from approximately 18:30 – 24:00 UTC on the 22nd, 23rd, and 24th of September. Blue dots represent the circulation center and the associated time. Yellow arrow denotes position of TC on the 22nd. White circle with red arc indicates position of TC on the 23rd and approximate location of eyewall convection. Black arrow denotes position of TC on the 24th. Color bar to the right denotes sea surface temperature.

GPS Sonde Locations
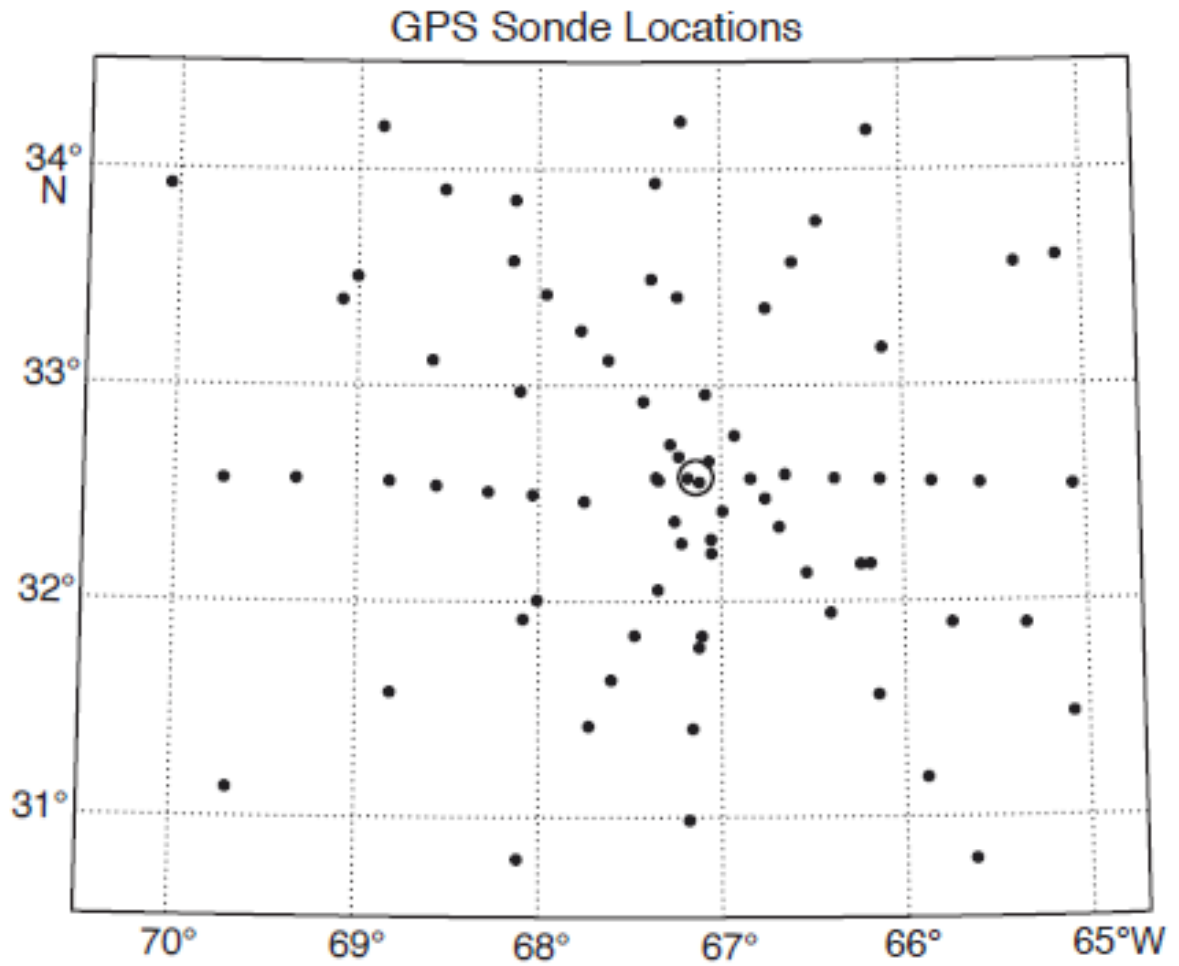
Fig. 3. Location of the GPS sondes on the 23rd of September relative to the circulation center. Center of the TC is the larger open circle.
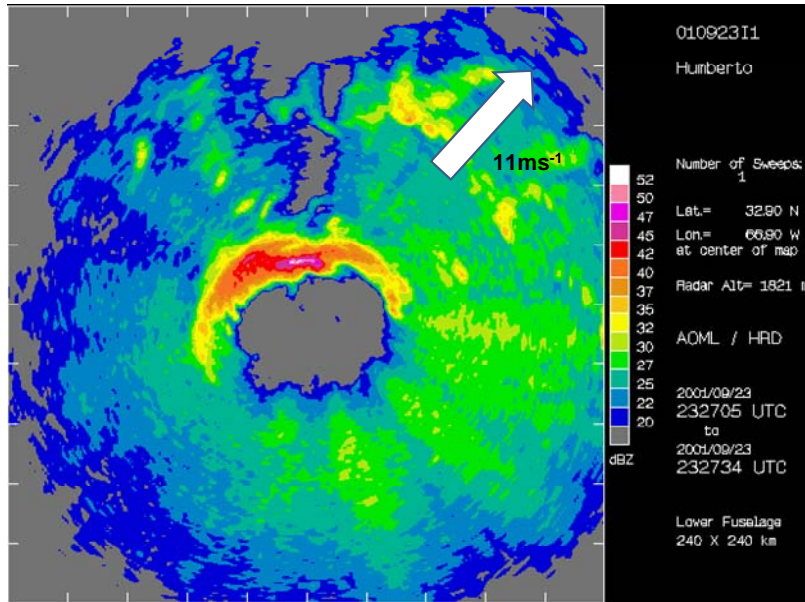
Fig 4. Plan view reflectivity image at 23:27 UTC of the eyewall of Humberto on September 23rd. Image is 240 x 240 km. White arrow displays shear direction and black print displays shear magnitude.
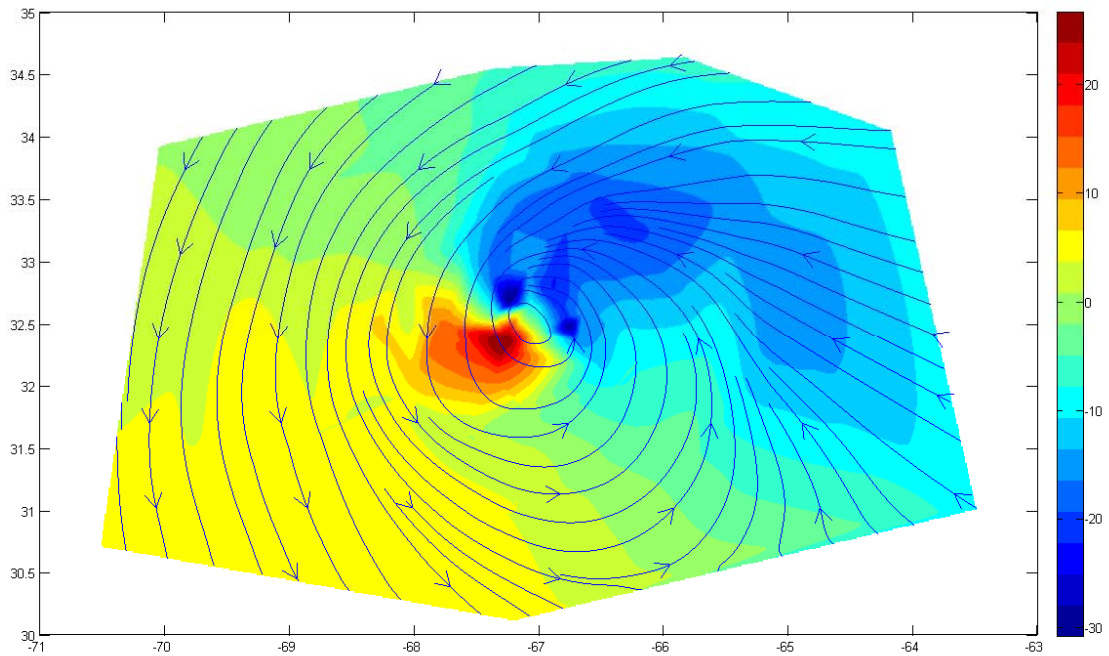
Fig. 5 Radial winds and streamlines at 250m. Color bar on right denotes magnitude of radial wind in m s-1.
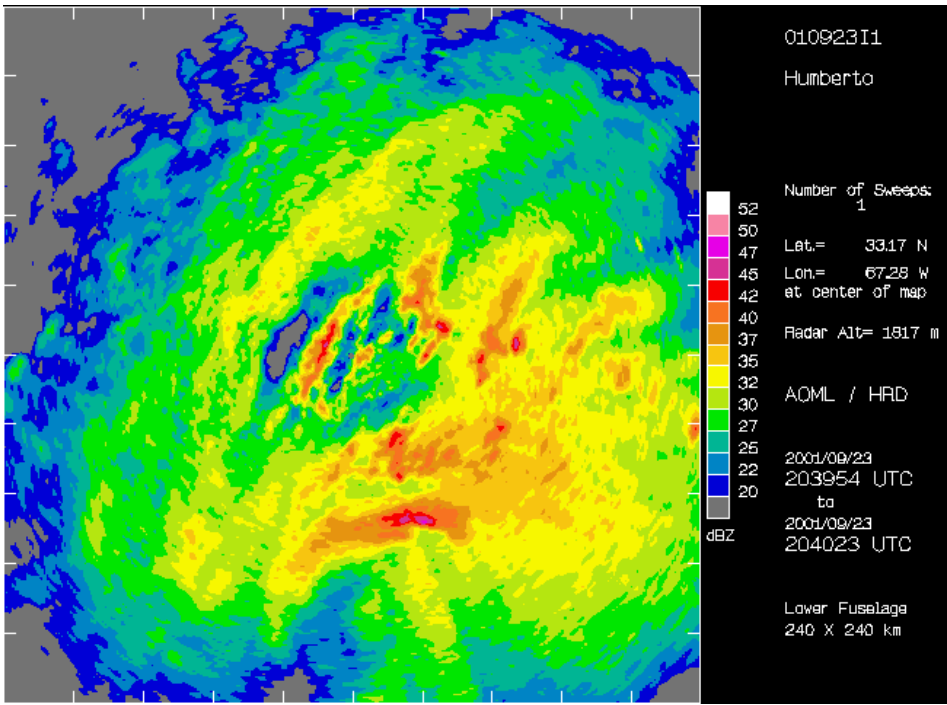
Fig 6. Plan view reflectivity image at 20:39 UTC of the eyewall of Humberto on September 23rd. Image is 240 x 240 km.
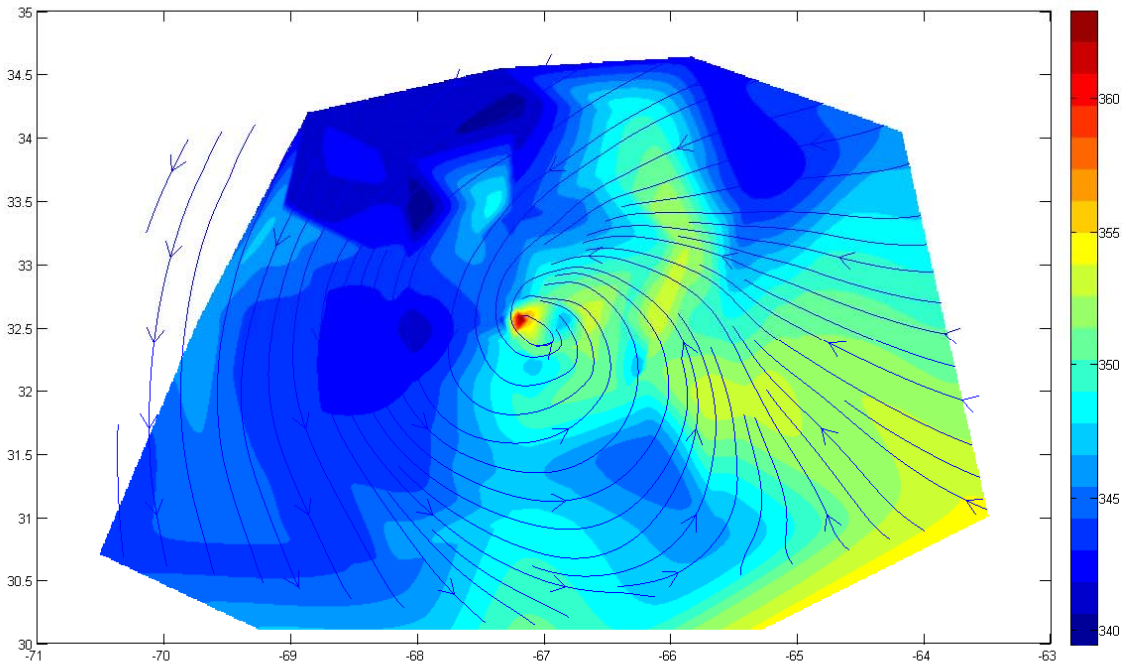
Fig. 7 Equivalent potential temperature and streamlines at 50m. Color bar to the right denotes equivalent potential temperatures in degrees Kelvin.
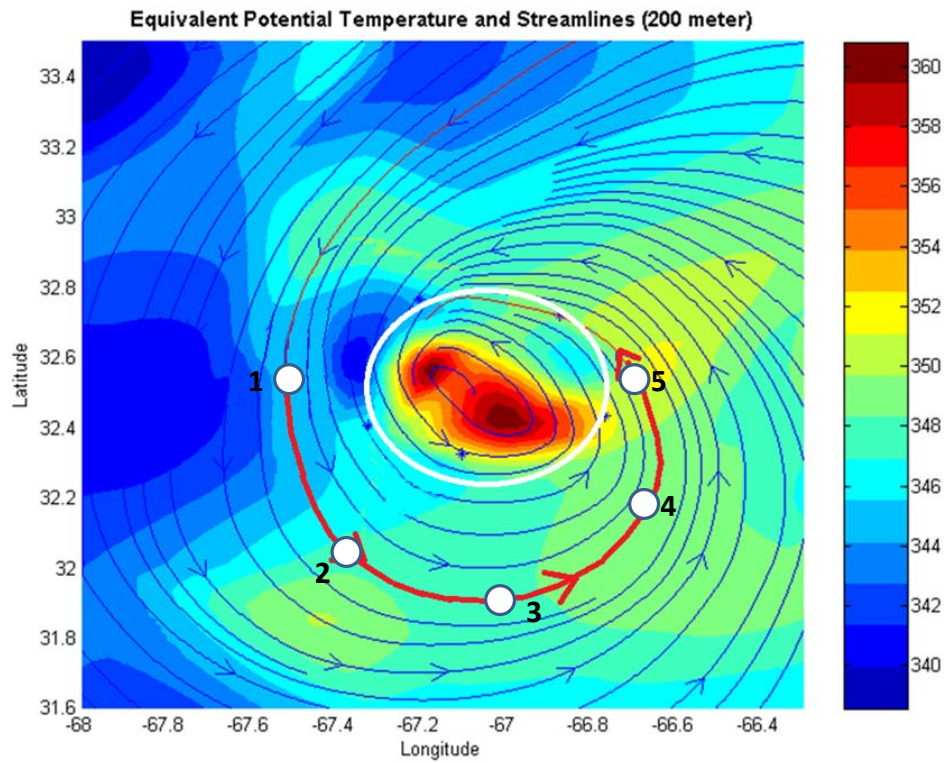
Fig. 8 Equivalent potential temperature and streamlines at 200m. Color bar to the right denotes equivalent potential temperatures in degrees Kelvin. White circle is the radius of maximum wind observed from the WP-3Ds. Red line with arrows shows approximate mean inflow trajectory for the boundary layer with the white dots and numbers denoting the position of each sounding taken for the energy budget.

A

Height (meters)

Equivalent Potential Temperature (K)

B

Height (meters)

Equivalent Potential Temperature (K)

C

Height (meters)

Equivalent Potential
Temperature (K)

D

Height (meters)

Equivalent Potential Temperature (K)
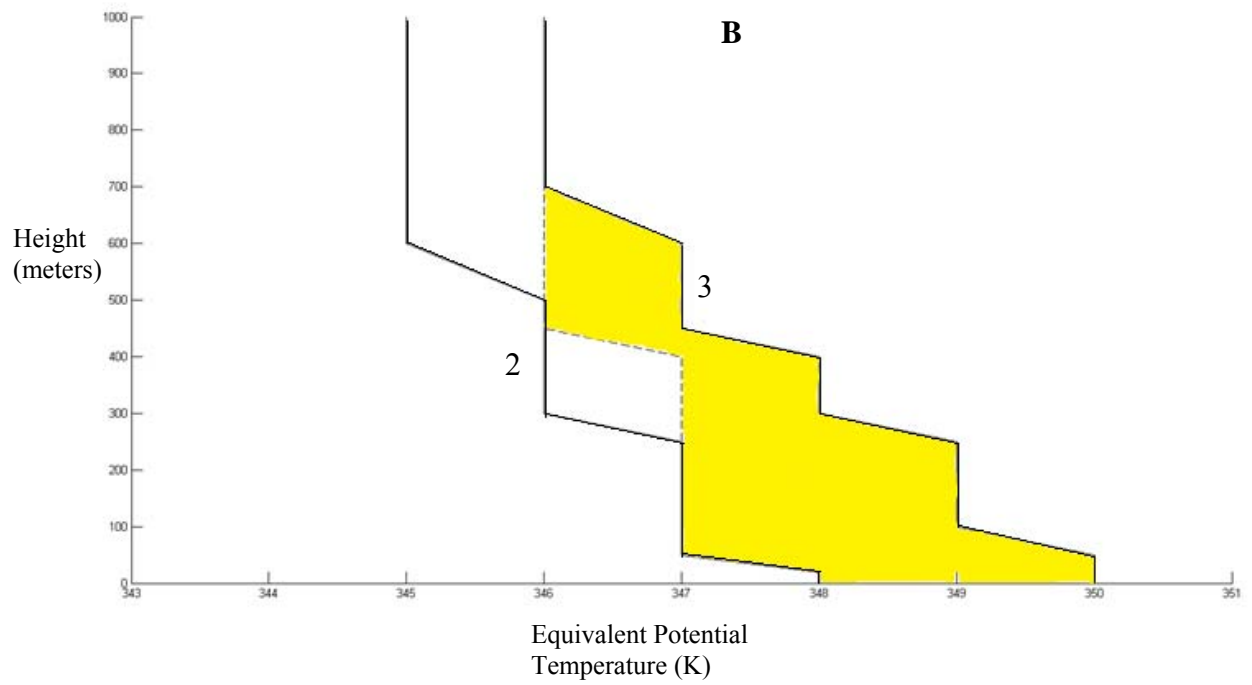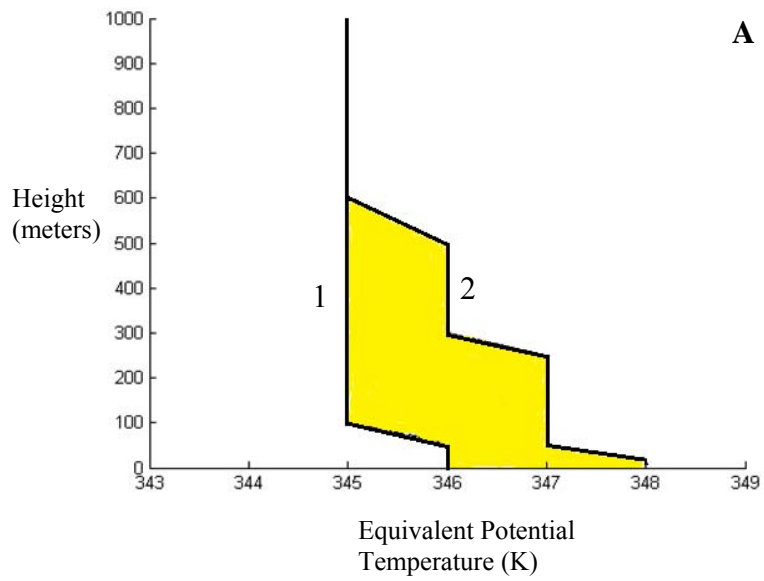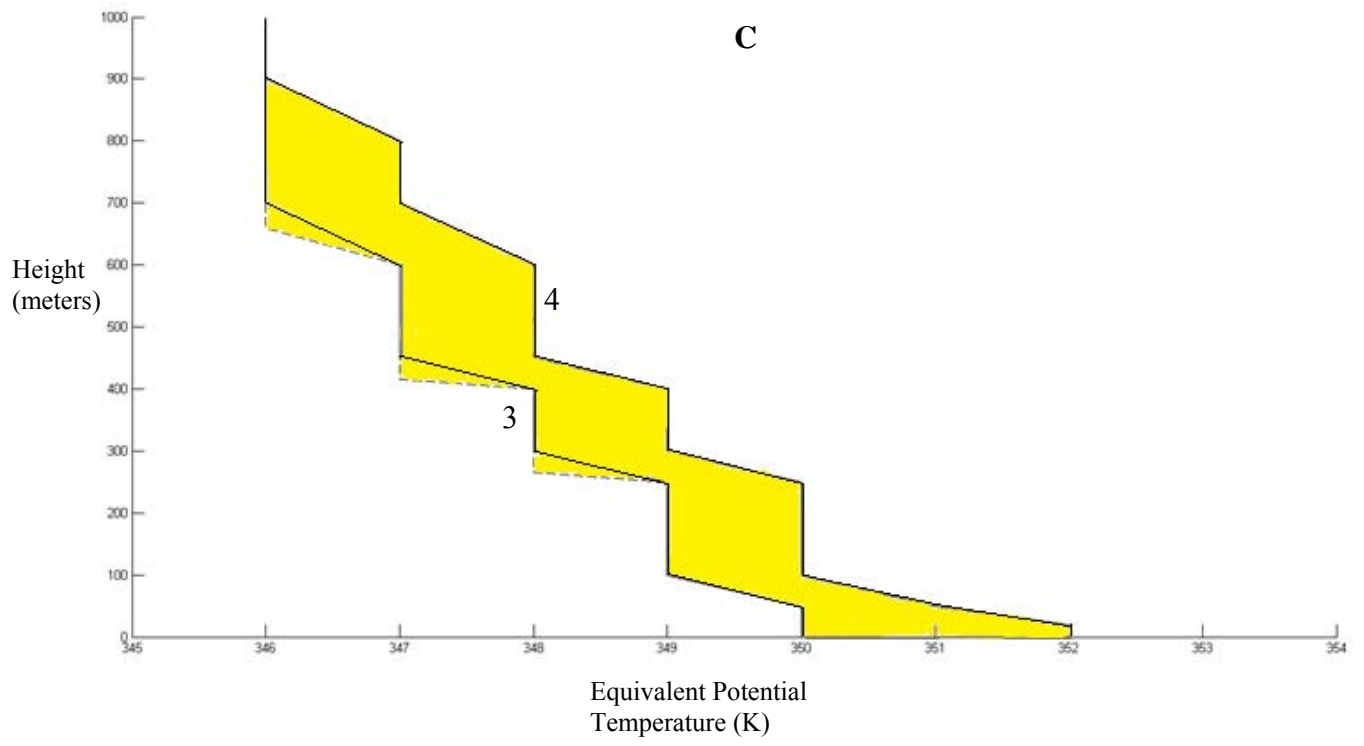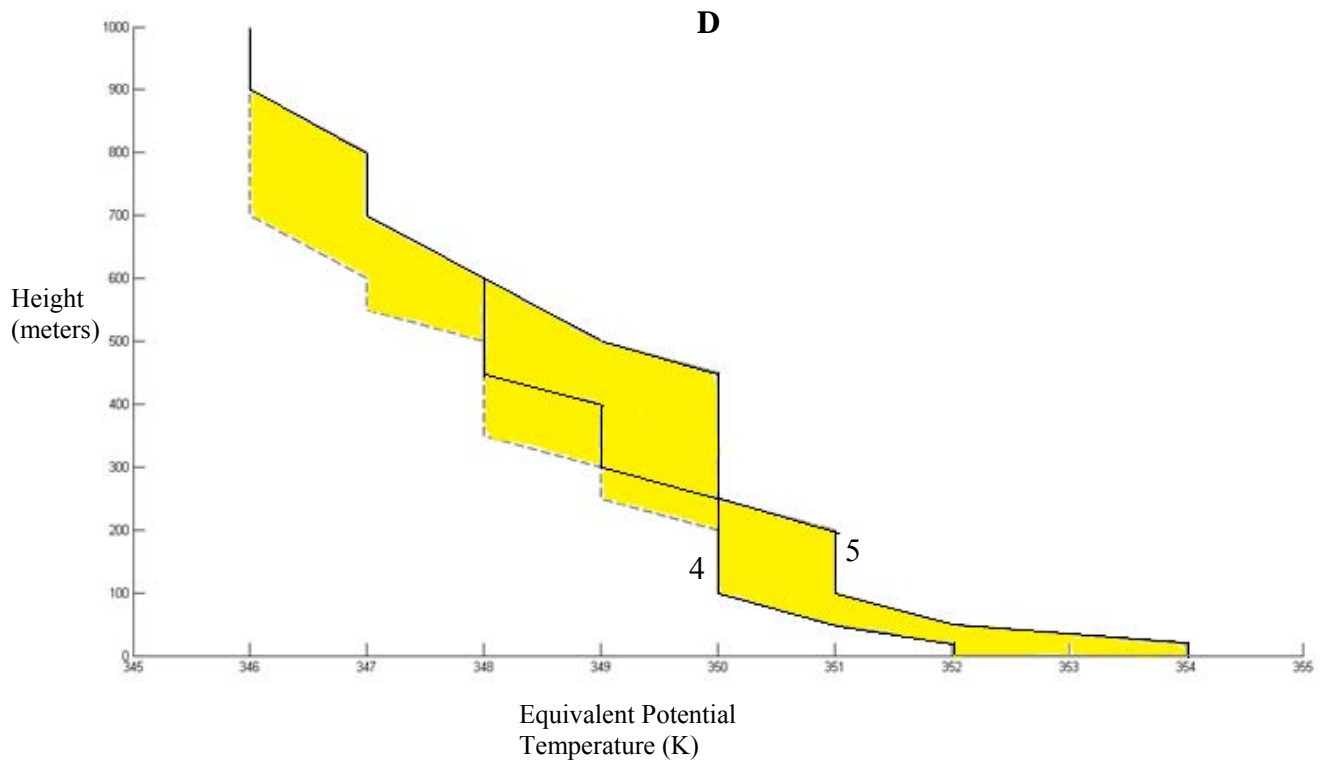
Fig. 9 Graph of equivalent potential temperature and height. Yellow shaded areas show total energy needed from the Humberto composites. (a) Sounding 1 to 2 (b) Sounding 2 to 3, dashed line shows net convergence and how it raises layers (C) Sounding 3 to 4, dashed line represents net divergence and how it lowers certain layers (D) Sounding 4 to 5, dashed lines show net divergence and how it lowers layers.